19th Australasian Fluid Mechanics Conference
Melbourne, Australia
8-11 December 2014

Centrifugal Instability over a Rotating Cone

Z. Hussain[1], S. J. Garrett[2] and S. O. Stephen[3]

[1]Division of Mathematics
Manchester Metropolitan University, Manchester M1 5GD, UK

[2]Department of Mathematics
University of Leicester, Leicester LE1 7RH, UK

[3]School of Mathematics and Statistics
University of New South Wales, Sydney NSW 2052, Australia

Abstract

In this study, we provide a mathematical description of the onset of counter-rotating circular vortices observed for a family of slender rotating cones (of half-angles 15°, 30° and 45°) in quiescent fluid. In particular, we apply appropriate scalings and apply a change of coordinates, accounting for the effects of streamline curvature. A combined large Reynolds number and large vortex wavenumber analysis is used to obtain an estimate for the asymptotic right-hand branch of neutral stability for the family of slender rotating cones. Existing experimental and theoretical studies are discussed which lead to the clear hypothesis of a hitherto unidentified convective instability mode that dominates within the boundary-layer flow over slender rotating cones. The mode manifests as Görtler-type counter-rotating spiral vortices, indicative of a centrifugal mechanism. Although a formulation consistent with the classic rotating-disk problem has been successful in predicting the stability characteristics over broad cones, it is unable to identify such a centrifugal mode as the half-angle is reduced. An alternative formulation is developed and the governing equations solved using both short-wavelength asymptotic and numerical approaches to independently identify the centrifugal mode. Our results confirm our earlier predictions pertaining to the existence of the new Görtler mode and capture the effects of the governing centrifugal instability mechanism. Meanwhile, favourable comparisons are drawn between numerical and asymptotic neutral stability curve predictions.

Introduction

This paper describes recent advances in the study of boundary-layer transition over rotating cones. In particular, we are concerned with the distinct convective instability mechanisms that dominate within the boundary layers over slender and broad rotating cones. Our interest in rotating cones is motivated by the flow around nose cones in aeroengine and spinning projectile applications. Here laminar–turbulent transition within the boundary layer can lead to significant increases in drag which has negative implications for fuel efficiency and control. Alternatively, turbulent flow can be encouraged as a means of heat transfer in situations where unwanted heat is generated, for example in re-entry. In any event, a complete understanding of the transition of such flows could lead to modifications in design and significant cost savings in aerospace technologies. It is clear that the linear-stability analyses presented here for cones rotating within incompressible and otherwise still fluids are of limited direct relevance in terms of these motivating applications. However, previous studies including [3, 5, 6] have shown that there is a close link between the rotating disk and cone problems in still fluid and axial flow. Hence, the current still fluid study forms an important stepping stone to analysing the more complex problem where axial flow is introduced. More generally, this work should be considered as a further step towards fully classifying the instability mechanics within the global class of boundary layer flows over rotating bodies. Indeed, studies of the effects of enforced axial flow over broad cones and disks have already been published, [1, 3, 5, 6].

Formulation

We use coordinate axes aligned with the spiral vortices and with origin O' placed at the local position of the analysis. As shown in figure 1, the $\hat{x}^*$-axis coincides with the direction of propagation of the spiral vortices aligned with the effective velocity direction. Alternatively, the y^*- and z^*-axes are mutually orthogonal and run in the tangential and surface-normal directions, respectively (where a * denotes a dimensional quantity in all that follows). The resulting coordinate system $(\hat{x}^*, y^*, z^*)$ rotates with the cone surface at constant angular frequency $\Omega^\star$. Importantly, the logarithmic spirals are directed such that the y^*-axis has a positive projection with respect to the direction of rotation of the cone. This requires that the $\hat{x}^*$-axis has positive projection onto the axis of rotation and the y^*-axis to have negative projection. The spiral vortices are orientated at an angle ϕ relative to the circle formed from the planar cross-sectional normal to the axis of rotation of the cone.

The governing dimensional Navier–Stokes equations are then derived in this co-ordinate system with appropriate scale factors. We non-dimensionalise lengths on a characteristic distance along the cone l^*, so that $\hat{x}^* = l^*\hat{x}$ and $y^* = l^* y$. Furthermore, we scale both logarithmic coordinates $\hat{x}$ and y, as well as the normal coordinate z^*, on the boundary-layer thickness, leading to the scaled coordinate system $(\check{x}, \bar{y}, \eta) = \mathrm{R}^{1/2}(\hat{x}, y, z)$ where R is the Reynolds number. This scaling enables the vortex structure in both logarithmic directions to be analyzed at the same order as the length scale in the surface-normal direction, which is another important difference from our previous formulation in [2]. We assume that the spiral waves are periodic in the effective velocity direction and introduce periodicity into the perturbation quantities of vortex $\check{x}$-wavenumber a and $\bar{y}$-wavenumber b. Scaling our perturbing quantities on the boundary-layer thickness, we introduce a perturbed flow of the form

$$\begin{aligned}\tilde{\mathbf{u}}^* &= \Omega^* l^* \sin\psi[\{x\tilde{U}(\eta;\phi), x\tilde{V}(\eta;\phi), \mathrm{R}^{-\frac{1}{2}}W\} \\ &+ \mathrm{R}^{-\frac{1}{2}}\{\tilde{u}(\eta), \tilde{v}(\eta), \tilde{w}(\eta)\}\exp(\mathrm{i}a\check{x} + \mathrm{i}b\bar{y})]. \qquad (1)\end{aligned}$$

where x is streamwise direction over the cone, scaled on l^* (see [2], for example). We note that these scalings remove ψ from the governing equations.

Full details of the mathematical derivation of the governing perturbation equations are given in [5] and we arrive at the governing stability equations stated in §5.2.1 [5]. We note that the governing equations are considerably more complicated than those

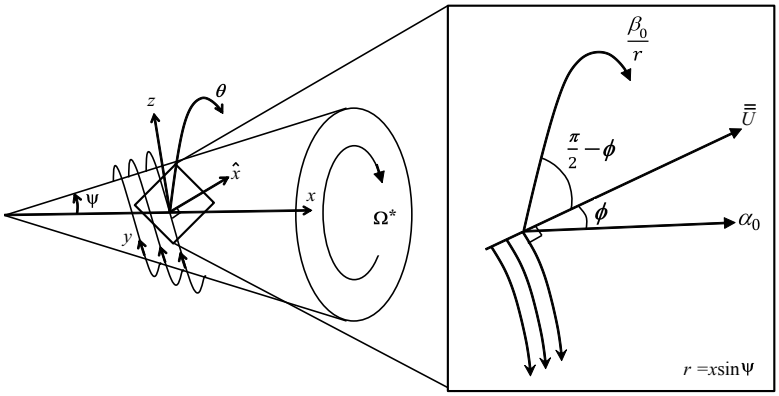

Figure 1. Diagram of spiral vortex instability of a rotating cone, showing conventional streamwise, aziumthal and surface-normal coordinates (x,θ,z) defined in [2], as well as the shifted logarithmic spiral coordinates $(\hat{x},\theta)$ (left). Also included is a detailed physical interpretation (right) showing the streamwise, azimuthal and effective velocity directions $\overline{\overline{U}}$. Note that α_0 and β_0/r refer to wavenumbers in the streamwise and azimuthal directions of the previous formulation [2], whereas the logarithmic spiral coordinate $\hat{x}$ coincides with the effective velocity direction $\overline{\overline{U}}$.

considered under the previous broad cone formulation [2] and this is a consequence of the different spatial scalings used here.

Asymptotic Analysis

The governing equations are solved to determine leading- and next-order estimates of a scaled Taylor number for neutrally-stable modes. The asymptotic approach follows [4] for the Taylor problem of flow between concentric rotating cylinders. Indeed, for slender rotating cones, ψ is sufficiently small that the formulation resembles that for flow moving axially over a rotating cylinder. The Taylor number in this formulation is given by

$$T = \frac{2\cot\psi\cos\phi}{\sin^5\psi}. \tag{2}$$

We consider it to be a function of ψ and parameterised by the particular ϕ under consideration. The expression is such that T increases with decreased ψ and can be considered as a measure of cone slenderness for particular ϕ. The Taylor number can be thought of as characterizing the importance of centrifugal forces relative to viscous forces, and is closely related to the Görtler number, which has been used to describe centrifugal instabilities, for example in fully developed and boundary layer flows by [4]. The perturbation quantities are expanded and we consider a WKB solution for small values of ε. Recall that $a = \varepsilon^{-1}$ with a the wavenumber in the $\check{x}$-direction. The dominant terms in the governing disturbance equations balance if we scale $T \sim \varepsilon^{-4}$ and $W/V \sim O(\varepsilon^{-2})$, resulting in

$$\begin{aligned}
\tilde{u} &= E(u_0(\eta)+\varepsilon u_1(\eta)+\varepsilon^2 u_2(\eta)+\ldots),\\
\tilde{v} &= \varepsilon^2 E(v_0(\eta)+\varepsilon v_1(\eta)+\varepsilon^2 v_2(\eta)+\ldots),\\
\tilde{w} &= E(w_0(\eta)+\varepsilon w_1(\eta)+\varepsilon^2 w_2(\eta)+\ldots),\\
T &= \varepsilon^{-4}(\lambda_0+\lambda_1\varepsilon+\lambda_2\varepsilon^2+\ldots),
\end{aligned}$$

where $\lambda = \lambda_0+\lambda_1\varepsilon+\lambda_2\varepsilon^2+\ldots$, $E = \exp\frac{\mathrm{i}}{\varepsilon}\int^{\varphi} K(\tau)\mathrm{d}\tau$ and $\varphi = \frac{\sin\psi}{h_1}\eta$.

After substitution of these expansions into the governing equations and some simplification owing to the assumption of small waveangle, we arrive at an eigenrelation at leading order which can be solved to give the scaled leading-order eigenvalue estimate. Following Hall's method, we seek to analyze vortex activity, which is found to be located at the wall near $\eta = 0$. We consider a thin layer about this location, which is of thickness

ψ	ϕ	$\bar{\lambda}_0$	$\bar{\lambda}_1$
15°	0°	1.6236	2.0769
30°	1°	1.6477	1.8567
	2°	1.6731	1.6389
	2.7°	1.6915	1.4887
	4°	1.7277	1.2162
	5°	1.7572	1.0146
	6°	1.7883	0.8221
	8°	1.8556	0.4747
45°	8.5°	1.8735	0.3979
	10°	1.9305	0.1991

Table 1. Leading- and first-order eigenvalue estimates of the scaled Taylor number for orientation angles as observed by Kobayashi & Izumi on cones with the stated half-angle.

$O(\varepsilon^{\frac{2}{3}})$, and expand the Taylor number to obtain a corresponding eigenvalue relation at first order. The mathematics is very involved and full details are given in [5]. In fact, we obtain an infinite sequence of eigenvalues $\{\lambda_{1n}\}$, corresponding to the zeros of an Airy function on the negative real axis. Combining the leading- and next-order solutions, the most dangerous instability mode has a scaled Taylor-number expansion given by

$$\bar{T} = \varepsilon^{-4}\left(\frac{1}{|\tilde{V}'(0)|}+\frac{2.34\times 3^{\frac{1}{3}}\varepsilon^{\frac{2}{3}}}{|\tilde{V}'(0)|}\left[\frac{\tilde{V}''(0)}{\tilde{V}'(0)}+\tilde{V}'(0)\cos\phi\right]^2+\ldots\right). \tag{3}$$

Numerical estimates of the leading- and first-order eigenvalues corresponding to the scaled Taylor number are shown in Table 1 for parameters in the experimental range observed by [8].

Numerical Analysis

While the numerical analysis reasonably consistent with the asymptotics, we make further approximations and manipulations to convert the disturbance equations into the governing fourth-order Orr–Sommerfeld (OS) equation for stationary disturbances within the system. We begin by neglecting terms arising from Coriolis and streamline-curvature effects and collate the resulting equations in terms of the normal perturbation velocity to form

$$\left[\mathrm{i}\left(\frac{\partial^2}{\partial\eta^2}-k^2\right)^2+Re\left(\alpha_1\tilde{U}+\beta_1\tilde{V}\right)\left(\frac{\partial^2}{\partial\eta^2}-k^2\right)\right.$$

ψ	ϕ	Re_c	$\alpha_{1,c}$
15°	0°	50	1.01
30°	2.7°	135	0.72
45°	8.5°	270	0.59

Table 2. Numerical calculations of the critical Reynolds numbers, Re_c, and critical vortex wavenumbers, $\alpha_{1,c}$, in the effective velocity direction for a range of small half-angle cones and corresponding vortex waveangles.

$$-Re\left(\alpha_1\frac{\partial^2\tilde{U}}{\partial\eta^2}+\beta_1\frac{\partial^2\tilde{V}}{\partial\eta^2}\right)\Bigg]\tilde{w}=0 \qquad (4)$$

where

$$\alpha_1=\frac{a\sin\psi}{Re},\qquad \beta_1=b\sin\psi,\qquad k=\sqrt{\alpha_1^2+\beta_1^2}, \qquad (5)$$

and $Re=x\sin\psi$ is the local Reynolds number, interpreted as the local non-dimensional radius of the cone surface from the axis of rotation. We relate this rotational Reynolds number, Re, to the conventional Reynolds number, R, using equation (8) of [8] to re-write the surface-curvature term, leading to

$$Re=\mathrm{R}^{\frac{1}{2}}\sqrt{1.616}. \qquad (6)$$

We solve the governing fourth-order perturbation equation (4) by employing an existing OS solver routine for the rotating cone, which has been modified to allow existing solutions for the OS neutral curve at specific values of ψ to be used in order to enable fast convergence when searching for neutral curves for the required values of ψ for slender cones. Numerical predictions of the critical Reynolds numbers and critical vortex wavenumbers for $\psi=15^\circ,30^\circ$ and 45° are shown in table 2. The results illustrate a decrease in the half-angle leads to a reduction in the critical Reynolds number, implying slender rotating cones represent the most unstable flow cases and cones of $\psi\leq 15^\circ$ harbour the most dangerous modes. This is corroborated by the critical vortex wavenumbers in the effective velocity direction, which increase for smaller values of ψ. Furthermore, while the results recover the findings of [8], importantly, at large Reynolds numbers and large vortex wavenumbers, we observe qualitative agreement with our asymptotic results.

Comparisons

Numerical analysis of the OS equation yields qualitatively correct predictions of the neutral stability curves, which increase in numerical accuracy as $Re\to\infty$ (see, for example, [3] for broad rotating cones). Hence, the OS results should recover the large vortex wavenumber asymptotics at high Reynolds number. Appropriate scalings are used, following [5] so that the Taylor number defined in equation (2) is linearly related to the rotational Reynolds number (see also [8]), leading to a relationship of the form

$$Re=\bar{T}\sqrt{1.616} \qquad (7)$$

for larger Reynolds number, Re, and large Taylor number, T. This such that increased $\bar{T}$ corresponds to reduced half-angle (for fixed ϕ). Comparisons with the Reynolds number Re predicted by the OS analysis against vortex wavenumber are shown in figures 2, 3 and 4 for $\psi=15^\circ,30^\circ$ and 45°, respectively. In each figure, we have computed asymptotic curves for $\phi=0^\circ,2.7^\circ$ and 8.5°, respectively, in order to compare with the most suitable basic flows from the OS analysis. These correspond to the theoretical values of ϕ presented in [8] and hence facilitate comparison with their results, as shown in [7] for $\psi=15^\circ$. We observe good qualitative agreement between the OS neutral curves and the asymptotic branches of the scaled

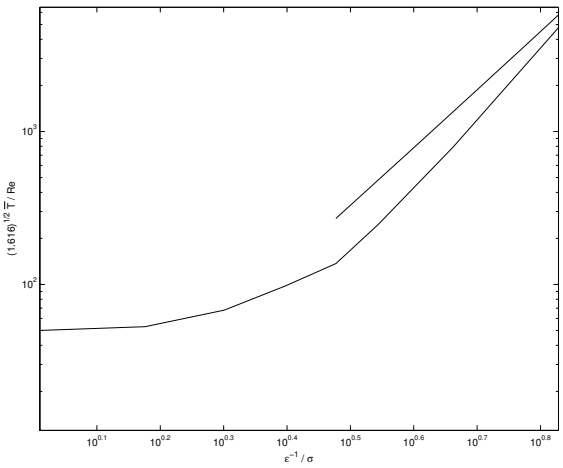

Figure 2. A comparison between the scaled effective asymptotic Taylor number $\bar{T}$ (above) and the Reynolds number Re predicted by the OS analysis (below), against vortex wavenumbers ε^{-1} and σ respectively, for $\psi=15^\circ,\phi=0^\circ$.

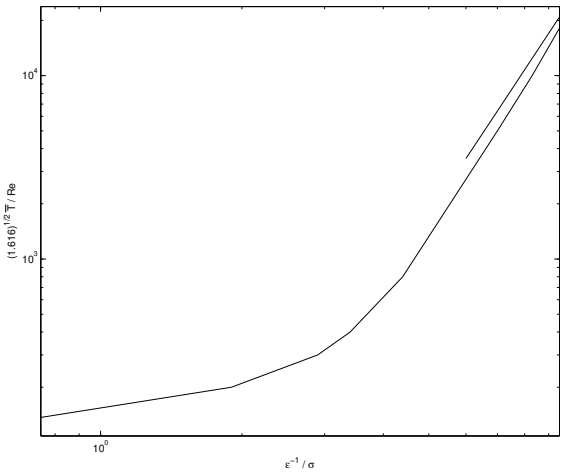

Figure 3. A comparison between the scaled effective asymptotic Taylor number $\bar{T}$ (above) and the Reynolds number Re predicted by the OS analysis (below), against vortex wavenumbers ε^{-1} and σ respectively, for $\psi=30^\circ,\phi=2.7^\circ$.

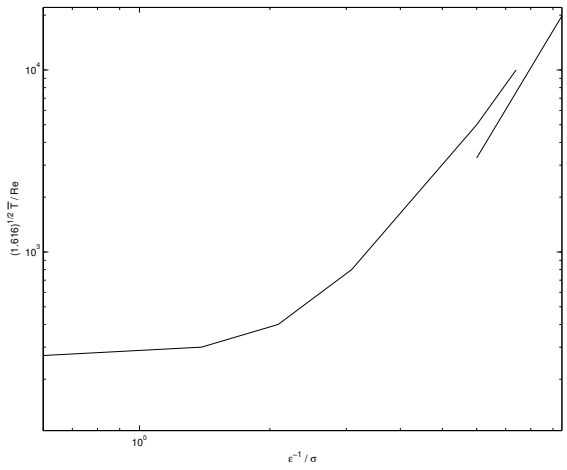

Figure 4. A comparison between the scaled effective asymptotic Taylor number $\bar{T}$ (below) and the Reynolds number *Re* predicted by the OS analysis (above), against vortex wavenumbers ε^{-1} and σ respectively, for $\psi = 45^\circ, \phi = 8.5^\circ$.

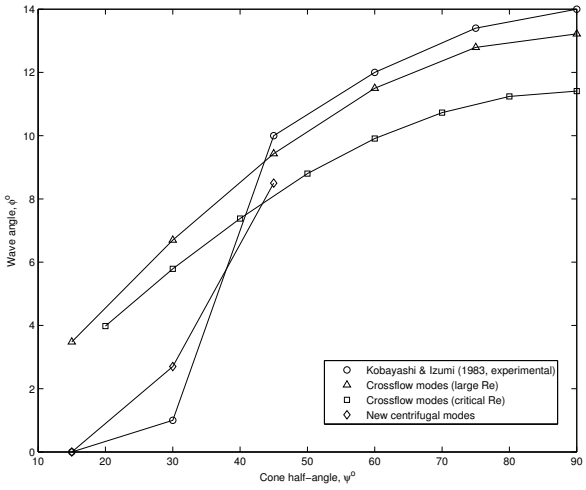

Figure 5. A comparison between experimental observations and theoretical predictions of the vortex orientation angle at the onset of instability, updated from [2]. The diagram illustrates the competing nature of the type I (crossflow) instability versus the new (centrifugal) instability modes, which dominate for slender half-angles and compare well with the experimental measurements in this regime.

effective Taylor number for $\psi = 15^\circ, 30^\circ$ and 45°. However, in particular, we notice that as ψ increases, the agreement between the asymptotics and numerics becomes more favourable for larger values of $\bar{T}$, further along the asymptotic branch, which is seen moving from figures 2 to 4.

Conclusions

In this paper we have motivated the hypothesis of a centrifugal-instability mode within the general class of rotating-cone boundary-layer flows. An alternative formulation that focuses on centrifugal effects has been developed and independent asymptotic and numerical analyses conducted to verify the existence of such a mode. The asymptotic analysis was used to identify the centrifugal mode, yielding an indication of the range of unstable wavenumbers against half-angle for large Reynolds numbers and large vortex wavenumbers. Meanwhile, the OS numerical analysis presented confirms existence of the centrifugal mode and reveals a reduction in the critical Reynolds number as well as an increase in the amplification rate with reduced half-angle, suggesting smaller values of ψ are destabilizing. Hence, for flow over a spinning cone surface with a relatively small half-angle, the centrifugal-instability mode may be interpreted physically as the most dangerous.

In conclusion, figure 5 shows a more complete view of the dependence of the vortex waveangle on ψ. A major finding of both the numerical and asymptotic studies in this parameter regime is that the centrifugal modes compare well with the experiments of [8], correcting the region where the crossflow instability theory presented in [2] was insufficient. Finally, while both the current study and [2] consider rotating cones in still fluid, the question of how introducing external parameters, such as an enforced axial flow, affects the interplay between the dominant instability modes remains. The crossflow instability for broader rotating cones in axial flow has been considered and discussed in [3]. Meanwhile, an investigation into the centrifugal instability for slender rotating cones within an imposed axial flow is ongoing and we shall report on this in the near future.

Acknowledgments

Partly supported by the EPSRC grant number EP/G061637/1.

References

[1] Garrett, S. J. and Peake, N., The absolute instability of the boundary layer on a rotating cone, *European. J. Mech. B.*, **26**, 2007, 344–53.

[2] Garrett, S. J., Hussain, Z. and Stephen, S. O., The crossflow instability of the boundary layer on a rotating cone, *J. Fluid Mech.*, **622**, 2009, 209–232.

[3] Garrett, S. J., Hussain, Z. and Stephen, S. O., Boundary-layer transition on broad cones rotating in an imposed axial flow, *AIAA Journal*, **48**, No. 6., 2010, 1184–1194.

[4] Hall, P., Taylor-Görtler vortices in fully developed or boundary-layer flows: linear theory, *J. Fluid Mech.*, **124**, 1982, 475–94.

[5] Hussain, Z., Stability and transition of three-dimensional rotating boundary layers, PhD thesis, University of Birmingham, 2010.

[6] Hussain, Z., Garrett, S. J. and Stephen, S. O., The convective instability of the boundary layer on a rotating disk in axial flow, *Phys. Fluids*, **23**, 2011, 1141108.

[7] Hussain, Z., Stephen, S.O. and Garrett, S.J., The centrifugal instability of a slender rotating cone, *Journal of Algorithms & Computational Technology*, Vol. 6, No. 1, 2012.

[8] Kobayashi, R. and Izumi, H., Boundary-layer transition on a rotating cone in still fluid. *J. Fluid Mech.* **127**, 1983, 353–64.

[9] Lingwood, R. J., Absolute instability of the boundary layer on a rotating disk, *J. Fluid Mech.*, **299**, 1995, 17–33.

[10] Malik, M. R., The neutral curve for stationary disturbances in rotating-disk flow, *J. Fluid Mech.*, **164**, 1986, 275–87.